

# EFFECTIVENESS FACTORS FOR REACTIONS BETWEEN VOLATILE AND NON-VOLATILE COMPONENTS IN PARTIALLY WETTED CATALYSTS

IOANNIS V. YENTEKAKIS and COSTAS G. VAYENAS†

Institute of Chemical Engineering and High Temperature Chemical Processes, University of Patras, Patras 26110, Greece

(Received 3 February 1986; accepted 21 July 1986)

**Abstract**—A steady state model is formulated to describe the reactions between one gaseous and two non-volatile components on partially wetted catalysts in a trickle-bed reactor. Unlike previous studies, the model does not assume a gaseous or liquid limiting reactant. The computed results show the effect of intraparticle and interphase mass transfer resistances as well as of wetting efficiency and number and location of wetted zones on catalyst performance. Maximum effectiveness factors are generally obtained with intermediate values of the wetting efficiency. The model is applied to a typical HDS process of heavy gas oil in trickle-bed reactors.

## 1. INTRODUCTION

The performance of catalyst pellets in trickle-bed reactors is affected significantly by interphase and intraparticle mass transfer resistances as well as by the extent of catalyst wetting (Satterfield, 1975; Colombo *et al.*, 1976; Morita and Smith, 1978; Gianetto *et al.*, 1978; Shah, 1979; Herskowitz *et al.*, 1979; Van Landeghem, 1980; Lee and Smith, 1982; Herskowitz and Smith, 1983). Criteria for assessing the importance of intra- and inter-phase heat and mass transfer resistances of pellets in a trickle-bed reactor and for determining the extent of pellet wetting have been developed (Lee and Smith, 1982). The role of wetting efficiency of catalyst pellets on catalyst performance depends critically on the nature of the limiting reactant.

For reactions in which the intrinsic rate is controlled by a non-volatile component, reduced wetting efficiency decreases the global rate. If the limiting reactant is in the gas phase, however, then a reduction in wetting efficiency tends to enhance catalyst performance (Herskowitz *et al.*, 1979; Ramachandran and Smith, 1979).

Typical values of wetting efficiencies in pilot scale and commercial trickle-bed reactor units are between 0.6 and 1 (Satterfield, 1975; Colombo *et al.*, 1976; Herskowitz *et al.*, 1979; Herskowitz and Smith, 1983). The dependence of wetting efficiency,  $f$ , on various operating parameters has been studied experimentally (Colombo *et al.*, 1976; Morita and Smith, 1978; Herskowitz *et al.*, 1979; Mills and Dudukovic, 1981; Herskowitz and Mosseri, 1983) and an expression of  $f$  in terms of the Reynolds, Froude and Weber numbers has been proposed and correlated well with existing experimental results (Mills and Dudukovic, 1981). Partial wetting of catalyst particles leads to non-uniform reactant concentrations around the external

surface and therefore conventional effectiveness factor expressions are not applicable.

Previous workers have computed overall effectiveness factors,  $\eta$ , for single reactions assuming either a gaseous or a non-volatile limiting reactant (Mills and Dudukovic, 1979; Ramachandran and Smith, 1979; Tan and Smith, 1980; Mills and Dudukovic, 1980; Herskowitz, 1981a; Herskowitz, 1981b; Goto *et al.*, 1981; Zheng *et al.*, 1984b). Analytical power series expressions have been obtained for the case of linear kinetics in various geometries (Herskowitz *et al.*, 1979; Herskowitz and Smith, 1983; Mills and Dudukovic, 1979; Mills and Dudukovic, 1980; Herskowitz, 1981b; Zheng *et al.*, 1984b) but evaluation of the power series coefficients from the resulting dual-series equations is difficult (Herskowitz and Smith, 1983). A powerful numerical method for coefficient evaluation and effectiveness factor computation has been developed (Mills and Dudukovic, 1979 and 1980). Approximate effectiveness factor expressions have also been proposed on the basis of the assumption that  $\eta$  can be expressed as a weighted average of the effectiveness factor  $\eta_L$  when the particle is completely wetted and of that when the particle is completely covered by gas (Ramachandran and Smith, 1979; Mills and Dudukovic, 1980; Tan and Smith, 1980; Goto *et al.*, 1981). Approximate and rigorously computed effectiveness factors have been compared for the case of first and  $n$ th order kinetics (Goto *et al.*, 1981) of the limiting reactant. Agreement is usually good for relatively large Thiele moduli (Mills and Dudukovic, 1980; Tan and Smith, 1980; Herskowitz, 1981b; Goto *et al.*, 1981). Previous theoretical studies have not addressed the problem of effectiveness factor computation when the concentrations of the gaseous and liquid reactants are comparable and the intrinsic rate depends on the both of them. This is the case in several important industrial trickle-bed reactor applications, such as the hydrodesulfurization of heavy petroleum fractions where the total concentration of sulfur containing

† Author to whom correspondence should be addressed.

compounds and of dissolved hydrogen are often comparable. In this case the rate is near first order in hydrogen for pressures below 140 bar and between first and second with respect to the sum of the sulphur containing compounds (Cecil *et al.*, 1968; Schuit and Gates, 1973; Rollmann, 1977; Gates *et al.*, 1979).

In the present communication we analyse the problem of reaction between a volatile and one or two non-volatile components in a partly wetted catalyst pellet without assuming any reactant to be reaction rate limiting. The reason for considering two non-volatile reactants is that this is the minimum number of pseudocomponents required to describe the substantially different reactivities of various sulphur containing compounds present in usual HDS reactor feedstocks (Schuit and Gates, 1973; Yitzhaki and Aharoni, 1977; Gates *et al.*, 1979). It should be noted that two pseudocomponents, each reacting with linear kinetics, suffice to describe the frequently observed second order dependence of total sulphur conversion on reactor LHSV (Cecil *et al.*, 1968; Schuit and Gates, 1973). As in previous studies the non-volatile reactants are assumed to diffuse into the catalyst pellet only through the liquid covered external surface. The gaseous reactant enters the pellet primarily through the so-called gas covered external surface, but also to a lesser extent through the wetted part of the external surface.

Both reaction rates were assumed to be first order in each of the two non-volatile components which are characterized by different reactivities. This is known to simulate well the apparent second order dependence of the HDS rate on the total sulphur content (Cecil *et al.*, 1968; Schuit and Gates, 1973).

The resulting equations were solved numerically using a finite difference approach. The effect was examined of the pertinent physicochemical parameters on catalyst performance. Particular emphasis was given to the wetting efficiency which, as expected, plays a dominant and interesting role, which is qualitatively different from that in the case of a single limiting reactant (Mills and Dudukovic, 1979; Mills and Dudukovic, 1980; Herskowitz, 1981a; Herskowitz, 1981b; Goto *et al.*, 1981; Zheng *et al.*, 1984b).

Previous studies have usually assumed one symmetric continuous polar wetted zone per catalyst pellet. The case of more than one wetted zone has been recently explored for the case of a single reactant with linear kinetics (Capra *et al.*, 1982; Ring and Missen, 1986). In the former case where the analysis was limited to a particular range of parameters corresponding to a hydrogenation reaction, the effect of increasing number of wetted zones was found to be negligible. Ring and Missen studied a wider range of parameters and found that the effectiveness factor can increase by as much as 40% when the number of wetted zones changes from one to four. In the present communication we examine the effect of the number as well as of the location of wetted zones by considering four different wetting patterns and by establishing the limiting behaviour when the number of wetted zones

becomes very large. Both the number and the location of wetted zones are found to have a significant effect on catalyst performance. Computed effectiveness factors typically increase by 100% as the number of wetted zones increases from one to infinity.

## 2. PROBLEM FORMULATION AND BASIC EQUATIONS

The porous catalytic pellet, assumed to be spherical, completely filled with liquid and partially wetted, is shown in Fig. 1. Assuming symmetric boundary conditions with respect to one axis of the sphere, one can express the fractional wetting coverage or wetting efficiency  $f$  in terms of the angles of the boundaries  $\Theta_f$ . In the case of one continuous polar wetted zone it is

$$f = (1 - \cos \Theta_f) / 2. \quad (1a)$$

Three other wetting cases were examined in order to study the effect of the number and location of wetted zones, as shown in Fig. 1: they can be called bipolar (b), equatorial (c) and bipolar-equatorial (d). The corresponding wetting efficiency expressions are

$$f = (1 - \cos \Theta_f) \quad (1b)$$

$$f = \cos \Theta_f \quad (1c)$$

$$f = (1 + \sin \Theta_f - \cos \Theta_f). \quad (1d)$$

Two reactions are assumed to take place in the pellet between a volatile component V and two non-volatile

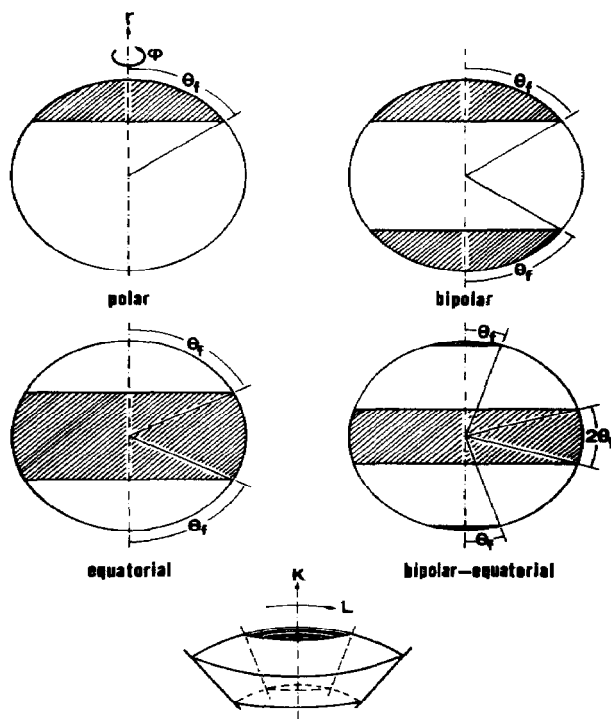


Fig. 1. Partially wetted spherical catalyst pellets and computational grid geometry.

components S1 and S2;



In the case of hydrodesulfurization (HDS) V stands for H<sub>2</sub> and S1 and S2 represent two sulphur containing pseudocomponents which differ considerably in reactivity for HDS, e.g. thiophene and a dibenzo thiophene (Nag *et al.*, 1979; Vrinat, 1983).

Assuming the pellet to be isothermal, which is usually a well justified assumption in most trickle-bed reactors (Herskowicz and Smith, 1983), one can write the following dimensionless mass balance equations for V, S1 and S2:

$$L[C_{S1}] = 9\xi_1 \Phi_1^2 r_1^* \quad (4)$$

$$L[C_{S2}] = 9\xi_2 \Phi_2^2 r_2^* \quad (5)$$

$$L[C_V] = 9\alpha_1 \zeta_1 \Phi_1^2 r_1^* + 9\alpha_2 \zeta_2 \Phi_2^2 r_2^* \quad (6)$$

$$\text{with } L[\ ] = \frac{1}{\rho^2} \frac{d}{d\rho} \rho^2 \frac{d[\ ]}{d\rho} + \frac{1}{\rho^2 \sin \Theta} \frac{d}{d\Theta} \sin \Theta \frac{d[\ ]}{d\Theta} \quad (7)$$

where  $\rho = r/(d_p/2)$ ,  $C_{S1} = \bar{C}_{S1}/\bar{C}_{S1,b}$ ,  $C_{S2} = \bar{C}_{S2}/\bar{C}_{S2,b}$ ,  $C_V = \bar{C}_v/\bar{C}_{v,eq}$

$$r_1^* = r_1(\bar{C}_{S1}, \bar{C}_v)/r_1(\bar{C}_{S1,b}, \bar{C}_{v,eq}),$$

$$r_2^* = r_2(\bar{C}_{S2}, \bar{C}_v)/r_2(\bar{C}_{S2,b}, \bar{C}_{v,eq})$$

$$\Phi_1^2 = (d_p/6)^2 r_1(\bar{C}_{S1,b}, \bar{C}_{v,eq})/D_{e,S1} \bar{C}_{v,eq}$$

$$\Phi_2^2 = (d_p/6)^2 r_2(\bar{C}_{S2,b}, \bar{C}_{v,eq})/D_{e,S2} \bar{C}_{v,eq}$$

$$\xi_1 = \bar{C}_{v,eq}/\bar{C}_{S1,b}, \xi_2 = \bar{C}_{v,eq}/\bar{C}_{S2,b},$$

$$\zeta_1 = D_{e,S1}/D_{e,v}, \zeta_2 = D_{e,S2}/D_{e,v}$$

The equilibrium volatile reactant concentration in the liquid phase  $\bar{C}_{v,eq}$  is defined as  $\bar{C}_{v,b}/H_v$  where  $H_v$  is the vapour-liquid equilibrium coefficient of species V.

In the case of one wetted zone the corresponding boundary conditions (BCs) are

$$\frac{dC_{S1}}{d\rho} = \text{finite}; \quad \rho = 0, 0 \leq \Theta \leq \pi \quad (8)$$

$$\frac{dC_{S1}}{d\rho} = Bi_{S1}(1 - C_{S1}); \quad \rho = 1, 0 \leq \Theta \leq \Theta_f \quad (9a)$$

$$\frac{dC_{S1}}{d\rho} = 0; \quad \rho = 1, \Theta_f < \Theta \leq \pi \quad (9b)$$

$$\frac{dC_{S2}}{d\rho} = \text{finite}; \quad \rho = 0, 0 \leq \Theta \leq \pi \quad (10)$$

$$\frac{dC_{S2}}{d\rho} = Bi_{S2}(1 - C_{S2}); \quad \rho = 1, 0 \leq \Theta \leq \Theta_f \quad (11a)$$

$$\frac{dC_{S2}}{d\rho} = 0; \quad \rho = 1, \Theta_f < \Theta \leq \pi \quad (11b)$$

$$\frac{dC_v}{d\rho} = \text{finite}; \quad \rho = 0, 0 \leq \Theta \leq \pi \quad (12)$$

$$\frac{dC_v}{d\rho} = Bi_{v,gs}(1 - C_v); \quad \rho = 1, 0 \leq \Theta \leq \Theta_f \quad (13a)$$

$$\frac{dC_v}{d\rho} = Bi_{v,gs}(1 - C_v); \quad \rho = 1, \Theta_f < \Theta \leq \pi \quad (13b)$$

where

$$Bi_{S1} = K_{ls,S1} d_p / 2D_{e,S1} \quad Bi_{S2} = K_{ls,S2} d_p / 2D_{e,S2}$$

$$Bi_{v,gs} = K_{gs,v} d_p / 2D_{e,v} \quad Bi_{v,gl} = K_{gl,v} d_p / 2D_{e,v}$$

Boundary conditions (8), (10) and (12) indicate that because of the asymmetry at  $\rho = 1$  it is in general  $dC_i/d\rho \neq 0$  at  $\rho = 0$ , i.e. the concentration minima of S1, S2 and V do not coincide with the centre of the pellet, as shown in Fig. 2 of the results sections. In the case of bipolar, equatorial and bipolar-equatorial wetting the angular constraints of BCs 9a, 9b, 11a, 11b, 13a and 13b change according to Fig. 1.

The effectiveness factors for reactions (2) and (3) can be computed from

$$\eta_1 = \frac{3}{2} \int_0^1 \int_0^\pi \rho^2 \sin \Theta r_1^* d\Theta d\rho \quad (14)$$

$$\eta_2 = \frac{3}{2} \int_0^1 \int_0^\pi \rho^2 \sin \Theta r_2^* d\Theta d\rho \quad (15)$$

An overall effectiveness factor may be defined from

$$\eta_{\text{overall}} = (\alpha_1 \zeta_1 \Phi_1^2 \eta_1 + \alpha_2 \zeta_2 \Phi_2^2 \eta_2) / (\alpha_1 \zeta_1 \Phi_1^2 + \alpha_2 \zeta_2 \Phi_2^2) \quad (16)$$

This effectiveness factor, which is a weighted average of  $\eta_1$  and  $\eta_2$ , expresses the ratio of the actual global rate of volatile component consumption to the rate that would prevail for infinitely fast intrapellet mass transfer.

### 2.1. Reaction kinetics

Equations (4)–(6) together with BCs (8)–(13) can be solved numerically for arbitrary kinetic expressions  $r_1$  and  $r_2$ . In this work mass action kinetics only have considered, i.e.

$$r_1 = K_1 \bar{C}_{S1} \bar{C}_v \quad (17)$$

$$r_2 = K_2 \bar{C}_{S2} \bar{C}_v \quad (18)$$

This was done because eqs (17) and (18) provide a satisfactory fit to the kinetic behaviour of several important reactions carried out commercially in trickle bed reactors, such as HDS of petroleum fractions on Co–Mo based catalysts (Kumar *et al.*, 1984). More complex Langmuir–Hinshelwood type rate expressions have also been proposed for HDS of model compounds (Satterfield and Roberts, 1968; Houalla *et al.*, 1978; Broderick and Gates, 1981; Singhal *et al.*, 1981) but these expressions are seldom used in industrial practice. The retarding effect of the product H<sub>2</sub>S on the rate of HDS is known to be important (Gates *et al.*, 1979; Vrinat, 1983) and should be taken into

account, particularly near the exit of the reactor. However few kinetic investigations have attempted to quantify this retarding effect by rate expressions containing  $P_{H_2S}$  explicitly. In most kinetic investigations (Yitzhaki and Aharoni, 1977; Rollmann, 1977; Nag *et al.*, 1979; Houalla *et al.*, 1980) the effect of  $H_2S$  is implicitly built into the experimentally extracted rate constants  $K_1$  and  $K_2$  of eqs (17) and (18).

## 2.2. Numerical solution

Equations (4)–(6) together with boundary conditions (8)–(13) were solved numerically using the finite difference method. The resulting set of  $3 \times K \times L$  nonlinear equations, where  $K$  and  $L$  are the numbers of grid points along the radial and angular direction respectively, were solved by means of the following iterative scheme: Arbitrary, usually zero, values were assigned to the nonlinear kinetic terms and the resulting set of  $3 \times K \times L$  linear equations was solved using Gauss elimination with pivoting for all  $3 \times K \times L$  concentrations which were then resubstituted into the kinetic terms. Convergence of all concentrations within 0.1% usually required 4–12 iterations. The number of grid points was varied in order to examine the accuracy of the results. In most runs it was found that  $K = 30$  and  $L = 12$  sufficed to provide satisfactory accuracy ( $\pm 1\%$ ) of the computed effectiveness factors.

## 3. RESULTS AND DISCUSSION

Figure 2 shows computed radial concentration profiles of the reactants in the catalyst particle for typical values of the Biot and Thiele numbers, one polar wetted zone and wetting efficiency  $f = 0.75$ . As expected, the minimum concentration of the volatile component  $V$  is found towards the liquid covered part of the pellet. The opposite is true for the concentrations of the two non-volatile components  $S1$  and  $S2$  where the minima are found at the gas covered surface.

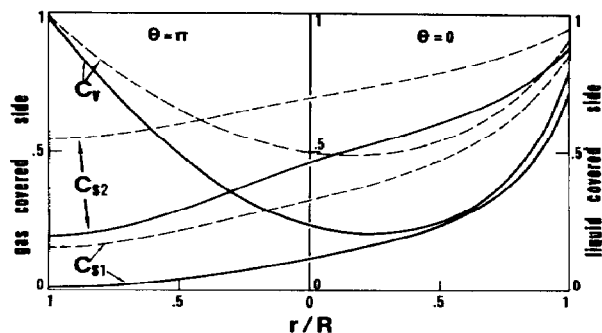


Fig. 2. Typical radial concentration profiles of nonvolatile reactants  $S1$ ,  $S2$  and volatile reactant  $V$  along the symmetry axis of the pellet, i.e.  $\Theta = 0$  and  $\pi$ ; solid lines:  $\Phi_1 = 2$ ,  $\Phi_2 = 1$ , dashed lines:  $\Phi_1 = 1$ ,  $\Phi_2 = 0.5$ ; other parameters:  $Bi_{S1} = Bi_{S2} = 10$ ,  $Bi_{v,gs} = 15$ ,  $Bi_{v,gs} = 100$ ,  $\xi_1 = \xi_2 = 1$ ,  $\zeta_1 = \zeta_2 = 0.5$ ,  $\alpha_1 = 1$ ,  $\alpha_2 = 3$ ,  $f = 0.75$ , polar wetting.

## 3.1. Limiting behaviour for negligible and severe mass transfer limitations

Interphase mass transfer plays a key role in global catalyst performance. This is shown in Fig. 3 where the effectiveness factor of one reaction  $\eta_1$  is plotted against the Thiele modulus  $\Phi_1$ . Curves labelled a correspond to the case of negligible interphase mass transfer resistance and were obtained by allowing all for Biot numbers to become infinitely large ( $> 10^4$ ). Curve  $a_1$  corresponds to complete wetting ( $f = 1$ ) and no side reaction ( $\Phi_2 = 0$ ). It gives the effectiveness factor  $\eta_{L,1}$  for a single bimolecular reaction in a spherical pellet with symmetric surface BCs and is proportional to  $\Phi_1^{-1}$  for large values of  $\Phi_1$ . Introducing partial wetting efficiency ( $f = 0.75$ ) and maintaining  $\Phi_2 = 0$  one obtains curve  $a_2$  which approximately conforms to  $\eta_1 = f\eta_{L,1}$ , except for  $\Phi_1 < 1$  as in the case of a monomolecular reaction (Colombo *et al.*, 1976; Gianetto *et al.*, 1978; Mills and Dudukovic, 1979; Herskowitz and Smith, 1983). Curve  $a_3$  corresponds to the same conditions with  $a_2$ , except  $\Phi_2$  is now non-zero and equal to 2. It can be seen that curves  $a_2$  and  $a_3$  coincide for large  $\Phi_1$  values, but  $a_3$  tends asymptotically to a value less than one for  $\Phi_1 \rightarrow 0$ . This is because the volatile reactant  $V$  is consumed by the second reaction even at vanishing  $\Phi_1$  values. Indeed as shown by curve  $a_4$  the effectiveness factor  $\eta_2$  of the second reaction is rather insensitive to changes in  $\Phi_1$ .

Curves on Fig. 3 labelled (b) correspond to the case of severe interphase mass transfer limitations and correspond to  $Bi_{S1} = Bi_{S2} = 0.1$ ,  $Bi_{v,gs} = Bi_{v,gl} = 0.2$ . Indices 1, 2, 3 and 4 of curves (b) correspond to the same  $f$  and  $\Phi_2$  conditions as with curves (a). The basic feature of curves (b) is that they become proportional to  $\Phi_1^{-2}$  for large  $\Phi_1$  values. In fact curve  $b_1$ , which

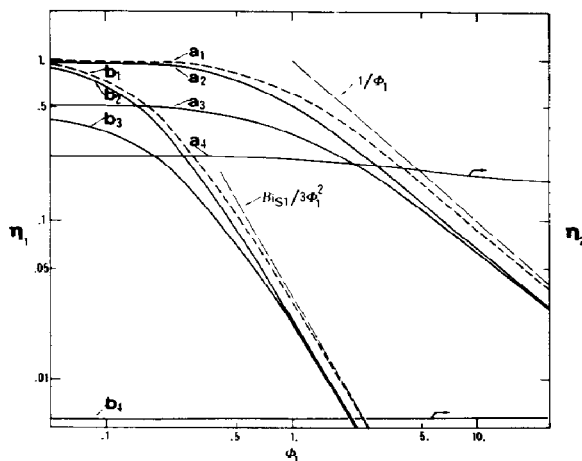


Fig. 3. Effect of Thiele modulus  $\Phi_1$  on the effectiveness factor  $\eta_1$  (curves  $a_1$ ,  $a_2$ ,  $a_3$ ,  $b_1$ ,  $b_2$ ,  $b_3$ ) and  $\eta_2$  (curves  $a_4$ ,  $b_4$ ) for negligible (curves a) and severe (curves b) external mass transfer limitations with  $\alpha_1 = 1$ ,  $\alpha_2 = 3$ ,  $\xi_1 = \xi_2 = 1$ ,  $\zeta_1 = \zeta_2 = 0.5$ . Curves (a):  $Bi_{S1} = Bi_{S2} = 10^4$ ,  $Bi_{v,gs} = Bi_{v,gl} = 2 \times 10^4$ ; curves (b):  $Bi_{S1} = Bi_{S2} = 0.1$ ,  $Bi_{v,gs} = Bi_{v,gl} = 0.2$ ; dashed curves correspond to complete wetting, all others to  $f = 0.75$ ; one polar wetted zone; see text for discussion.

corresponds to complete wetting, practically coincides with  $\eta_1 = Bi_{S1}/3\Phi_1^2$  for  $\Phi_1$  values larger than one. This result is identical to that obtained for first order reactions in spherical pellets with symmetric surface BCs.

Introduction of partial wetting efficiency  $f = 0.75$  results in curves  $b_2(\Phi_2 = 0)$  and  $b_3(\Phi_2 = 2)$ , which show that the approximation  $\eta_1 = f\eta_{L,1}$  is again valid for  $\Phi_1 > 1$ .

### 3.2. Effect of wetting efficiency

Figures 4 and 5 show the effect of wetting efficiency on catalyst performance for one polar wetted zone when interphase mass transfer of the non-volatile reactants is relatively slow with respect to the interphase mass transfer of the gaseous component. Under these conditions the liquid reactants tend to become rate

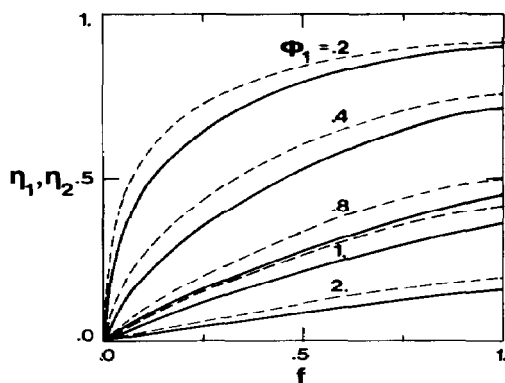


Fig. 4. Effect of wetting efficiency on effectiveness factors  $\eta_1$ ,  $\eta_2$  for various values of  $\Phi_1$ ,  $\Phi_2$  and fast mass transfer of the volatile component;  $Bi_{S1} = Bi_{S2} = 10$ ,  $Bi_{v,gs} = 20$ ,  $Bi_{v,gs} = 100$ ,  $\zeta_1 = 1.6$ ,  $\zeta_2 = 1$ ,  $\zeta_1 = \zeta_2 = 0.5$ ,  $\alpha_1 = 3$ ,  $\alpha_2 = 1$ ,  $\Phi_2 = \Phi_1$ , polar wetting.

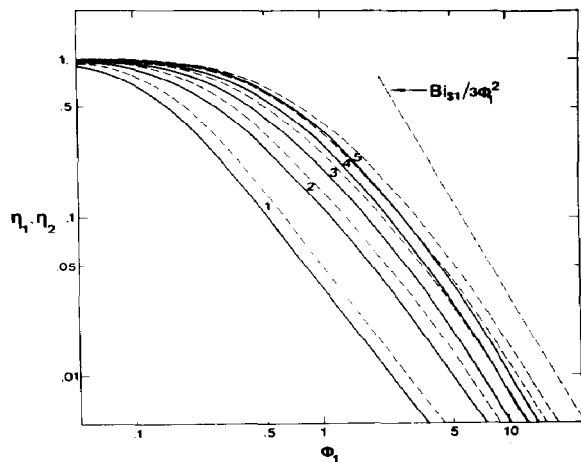


Fig. 5. Effectiveness factor dependence on Thiele modulus for fast mass transfer of the volatile component. Curves labelled 1-5 correspond to  $f = 0.067, 0.25, 0.5, 0.75$  and 1.0 respectively; conditions as in Fig. 4.

limiting and the situation is qualitatively similar to that analysed for single reactions with first or  $n$ th order kinetics (Mills and Dudukovic, 1979; Herskowitz, 1981b; Goto *et al.*, 1981) i.e. the effectiveness factors  $\eta_1$  and  $\eta_2$  are monotonically increasing functions of  $f$ . In these and in following figures the effectiveness factor of the more reactive component  $\eta_1$  is shown by solid curves, while the corresponding  $\eta_2$ , which is always greater than  $\eta_1$ , is represented by dashed curves. The overall effectiveness factor is not shown, since it is always bracketed between  $\eta_1$  and  $\eta_2$  and can be readily computed from equation (16).

As shown in Fig. 4 the approximation  $\eta_i = f\eta_{L,i}$  ( $i = 1, 2$ ) can provide a reasonable estimate of  $\eta_i$  only for  $\Phi_i$  exceeding unity. However the practical usefulness of this simplifying approximate expression is further diminished by the fact that, as shown in section 3.5, the number and location of the wetted zone(s) has a significant effect on  $\eta_i$ , thus the value of  $f$  by itself cannot provide a complete description of the wetting pattern. Figure 5 shows the effect of  $\Phi_i$  on  $\eta_i$  for constant values of  $f$ . For large  $\Phi_i$  values the effectiveness factors  $\eta_i$  become proportional to  $1/\Phi_i^2$ . This is because of the relatively small Biot numbers used in these computations. The fact that  $\eta_1$  and  $\eta_2$  do not reach the limiting values of  $f Bi_{S1}/\Phi_1^2$  and  $f Bi_{S2}/\Phi_2^2$  for large  $\Phi_i$ , as they would in the case of single first order reactions, is due to the consumption of the volatile component by both reactions.

When the interphase mass transfer resistances of the gaseous and non-volatile components are comparable and the gaseous component is transferred primarily via the gas covered particle surface, then the effectiveness factor exhibits a maximum at intermediate  $f$  values. This is shown in Fig. 6 which also demonstrates that the optimum wetting efficiency is rather insensitive to changes in the Thiele moduli.

The optimum wetting efficiency depends strongly on the interphase mass transfer resistance of the volatile component at the liquid covered particle surface. This

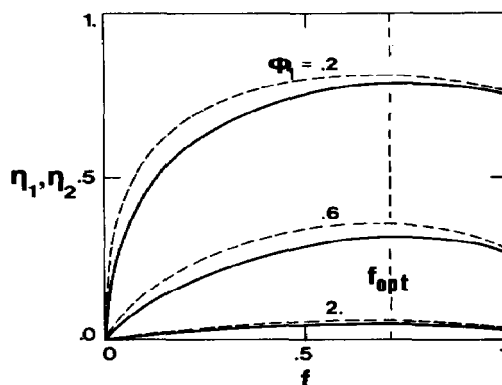


Fig. 6. Effect of wetting efficiency on catalyst performance for slow mass transfer of the volatile component on the wetted part of the catalyst surface;  $Bi_{S1} = Bi_{S2} = 10$ ,  $Bi_{v,gs} = 1$ ,  $Bi_{v,gs} = 50$ ,  $\zeta_1 = 1.6$ ,  $\zeta_2 = 1$ ,  $\zeta_1 = \zeta_2 = 0.5$ ,  $\alpha_1 = 3$ ,  $\alpha_2 = 1$ ,  $\Phi_2 = \Phi_1$ , polar wetting.

is shown in Fig. 7 which demonstrates that the optimum value of the wetting efficiency  $f_{opt}$  increases with increasing  $Bi_{v, gls}$ . Under similar conditions  $\eta_{max}$  and  $f_{opt}$  have both been found to be insensitive to  $Bi_{v, gs}$  provided the latter exceeds  $Bi_{v, gls}$ . This is explained by noticing that the volatile component enters the pellet primarily via the gas covered part of the external surface; since  $Bi_{v, gs}$  is sufficiently large the rate of mass transfer of the gaseous reactant is determined primarily by the value of  $f$ .

### 3.3. Effect of $Bi_{v, gs}$ and $Bi_{v, gls}$

For fixed values of the wetting efficiency  $f$  increasing  $Bi_{v, gls}$  enhances catalyst performance. This is shown in Fig. 8. For the same values of parameters the effect of increasing  $Bi_{v, gs}$  is less pronounced. The effect would be significant only for small values of the bulk concentration of the gaseous reactant.

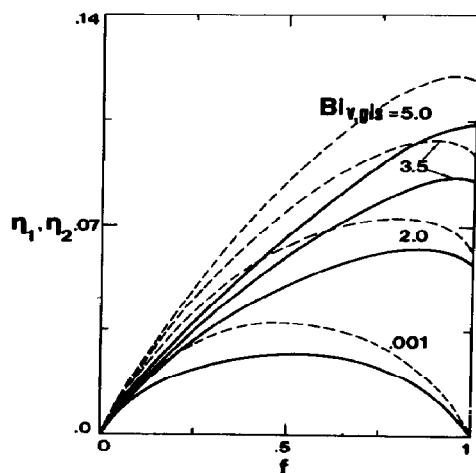


Fig. 7. Effect of gas-liquid-solid mass transfer coefficient of volatile component  $Bi_{v, gls}$  on the optimum wetting efficiency  $f_{opt}$ ;  $\Phi_1 = \Phi_2 = 2$ , other conditions as in Fig. 6.

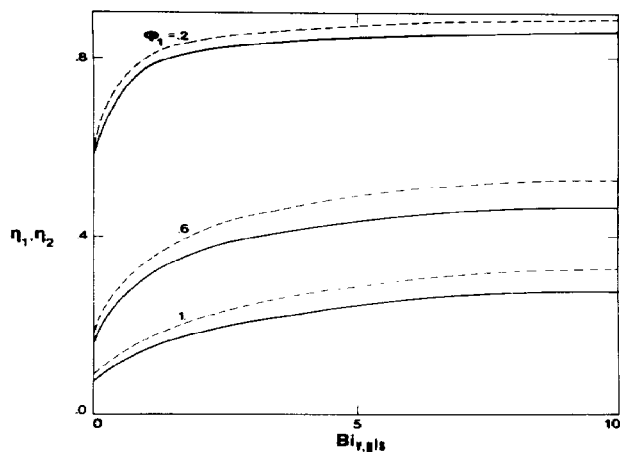


Fig. 8. Effectiveness factors  $\eta_1, \eta_2$  vs  $Bi_{v, gls}$  for various values of  $\Phi_1 = \Phi_2$ ;  $Bi_{S1} = Bi_{S2} = 10$ ,  $Bi_{v, gs} = 15$ ,  $\xi_1 = 1.6$ ,  $\xi_2 = 1$ ,  $\zeta_1 = \zeta_2 = 0.5$ ,  $\alpha_1 = 3$ ,  $\alpha_2 = 1$ ,  $f = 0.75$ , polar wetting.

### 3.4. Effect of bulk concentrations of the reactants

Figure 9 shows the effect of varying the ratio of the bulk concentrations of the volatile and non-volatile reactants for various values of the wetting efficiency  $f$ . For large values of  $\xi_1$  and  $\xi_2$  the liquid reactants are rate limiting, therefore catalyst performance is enhanced by increasing  $f$  values.

However when  $\xi_1$  and  $\xi_2$  are such that the non-volatile reactants are in excess of the stoichiometric requirement, then  $\eta_1$  (and  $\eta_2$ ) pass through a maximum with increasing  $f$ . As shown in Fig. 9,  $f$  values which correspond to the maxima decrease with decreasing  $\xi_1$  and  $\xi_2$ . This is because to the left of the maxima the rate is limited by the supply of the non-volatile components while mass transport of the gaseous reactant is rate limiting at higher  $f$  values.

### 3.5. Effect of number and location of wetted zones

The number and the location of wetted zones both have significant effects on catalyst performance as shown in Fig. 10. A similar conclusion has been reached for the case of a single first order reaction (Ring and Missen, 1986). Figure 10 shows that for the case of a single wetted zone polar wetting is always inferior to equatorial wetting. Bipolar wetting is superior than equatorial wetting for  $f > 0.5$  but becomes inferior for  $f < 0.5$ . This shows that the location of the wetting zones is equally important to their number. Of the four wetting patterns examined the bipolar-equatorial wetting gives the highest catalyst performance.

The above observations can be rationalized by considering that an increase in the number of wetting zones generally enhances the gas-liquid reactant contact. A qualitative measure of the gas-liquid contact efficiency is the length of the boundaries of the wetted zones. For the four cases examined and for any fixed  $f$  value the boundary length is minimum for polar wetting and maximum for bipolar-equatorial wetting, in qualitative agreement with the corresponding effectiveness factors. Furthermore for  $f < 0.5$  the bound-

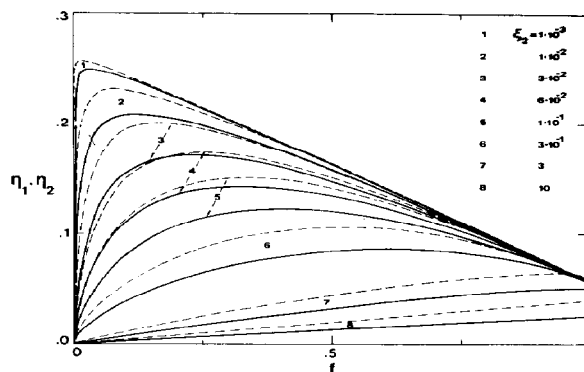


Fig. 9. Effect of the equilibrium liquid phase ratio of volatile to non-volatile reactant concentrations  $\xi_1, \xi_2$  on catalyst performance and optimum wetting efficiency;  $\Phi_1 = \Phi_2 = 2$ ,  $Bi_{S1} = Bi_{S2} = 10$ ,  $Bi_{v, gls} = 2$ ,  $Bi_{v, gs} = 50$ ,  $\zeta_1 = \zeta_2 = 0.5$ ,  $\alpha_1 = 3$ ,  $\alpha_2 = 1$ ,  $\xi_1 = 1.6$ ,  $\xi_2$ , polar wetting.

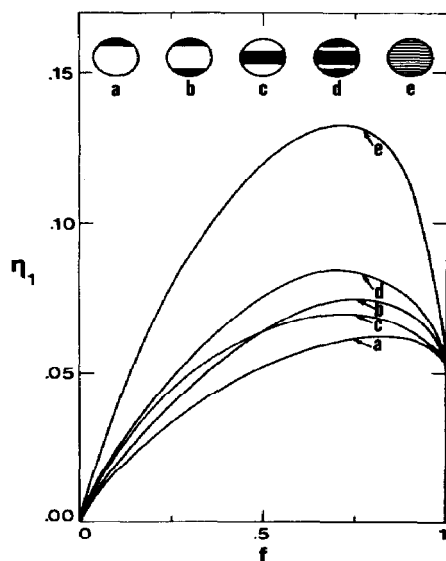


Fig. 10. Effect of wetting geometry on catalyst performance. Wetted zones shown in black.  $Bi_{S1} = Bi_{S2} = 10$ ,  $Bi_{v, gls} = 2$ ,  $Bi_{v, gs} = 50$ ,  $\zeta_1 = 1.6$ ,  $\zeta_2 = 1$ ,  $\zeta_1 = \zeta_2 = 0.5$ ,  $\alpha_1 = 3$ ,  $\alpha_2 = 1$ ,  $\Phi_1 = \Phi_2 = 2$ .

ary length for bipolar wetting is smaller than the boundary length for equatorial wetting. The opposite is true for  $f > 0.5$  in good qualitative agreement with the corresponding effectiveness factor behaviour (Fig. 10).

Since the single polar wetting zone model is always characterized by the smallest boundary length among all possible wetting geometries for any fixed wetting efficiency  $f$ , it is reasonable to conclude that the single polar wetting geometry, which was used in all previous studies, provides the lowest estimate of catalyst performance.

Figure 10 also shows the best catalyst performance (curve e) which can be obtained in the limiting case of an infinite number of wetting zones which are uniformly distributed on the external surface of the pellet and have a total surface area equal to a fraction  $f$  of the total area of the pellet surface. This limiting case was computed by setting  $Bi'_{S1} = f Bi_{S1}$ ,  $Bi'_{S2} = f Bi_{S2}$ ,  $Bi'_{v, gls} = f Bi_{v, gls} + (1-f) Bi_{v, gs}$  in BCs (9), (11) and (13) for  $0 \leq \Theta \leq \pi$ .

### 3.6. Application to HDS of heavy gas oil

Hydrodesulphurization of heavy gas oil (HGO) is carried out in trickle-bed reactors using  $\gamma\text{-Al}_2\text{O}_3$  supported  $\text{CoO-MoO}_3$  catalyst particles, typically 0.3–0.08 cm in diameter. Important information about industrial operating conditions can be found in the reviews of (Schuit and Gates, 1973; Satterfield, 1975). Typical superficial mass velocities are of order 1–10  $\text{kg/m}^2 \text{s}$  for the liquid and 0.2  $\text{kg/m}^2 \text{s}$  for hydrogen. Most industrial reactors operate in the trickle-flow (gas continuous) regime but operation in the pulse-flow regime is also possible (Satterfield, 1975;

Gianetto *et al.*, 1978; Satterfield *et al.*, 1978; Herskowitz and Smith, 1983).

The hydrodynamics of trickle-bed reactors have been reviewed recently (Talmor, 1977; Gianetto *et al.*, 1978; Herskowitz and Smith, 1983).

The present steady state model is applicable to the case of the trickle-flow regime where the wetting efficiency of individual particles can be reasonably assumed to remain constant with time. However in the pulse-flow regime a dynamic model would be required to take into account the periodic variation of the wetting efficiency of individual particles. Work along these lines is currently in progress.

### 3.7. Parameter estimation

The values of the operating parameters used in the numerical simulation are shown in Table 1. The sulphur containing compounds were simulated by an equimolar mixture of a reactive component S1 and a less reactive component S2. Dibenzothiophene (DBT) was chosen to simulate S2 since it is one of the most abundant less reactive sulphur compounds found in HGO (Houalla *et al.*, 1978; Nag *et al.*, 1979; Houalla *et al.*, 1980; Singhal *et al.*, 1981) and since the kinetics of DBT hydrodesulphurization have been studied extensively (Rollmann, 1977; Houalla *et al.*, 1978; Nag *et al.*, 1979; Houalla *et al.*, 1980; Broderick and Gates, 1981; Singhal *et al.*, 1981; Kumar *et al.*, 1984; Broderick, 1980) thiophene (TH) was chosen to represent the more active pseudocomponent S1. Its activity is approximately 20 times higher than that of DBT (Nag *et al.*, 1979; Vrinat, 1983) and the kinetics of its hydrodesulphurization have been studied in detail (Satterfield and Roberts, 1968). The HDS reactivity of various sulphides, bisulphides and mercaptans found in HGO is very high under typical reactor operating conditions. As a result their conversion is almost complete at very short contact times and therefore these compounds play a very limited role in HDS reactor modelling and design.

Calculated dimensionless parameter values required for the numerical simulation are shown in Table 2. Parameter estimation details are given in Appendix A. Computed effectiveness factors shown in Fig. 11 for two typical ratios of bulk reactant concentrations

Table 1. Operating parameters

$T = 345^\circ\text{C}$	$P = 90 \text{ bar}$
Mass velocities HGO: 2.1 $\text{kg/m}^2 \text{s}$	$\text{H}_2$ : 0.12 $\text{kg/m}^2 \text{s}$
Catalyst: Houdry HDS-16A $d_p = 25 \text{ mm}$ $\varepsilon = 0.5$	
$M_{\text{HGO}} = 210$	$M_{\text{S1}} = 84$ (thiophene)
	$M_{\text{S2}} = 184$ (DBT)
$d_{\text{HGO}} = 600 \text{ kg/m}^3$	$\mu_{\text{HGO}} = 0.16 \times 10^{-3} \text{ Pa.s}$
Sulphur content: 2.2 wt %	

Table 2. Computed dimensionless groups

$Bi_{S1} = 148$	$Bi_{S2} = 177$	$\zeta_1 = \zeta_2 = 1.57\text{--}0.75$
$Bi_{v, gls} = 50$	$Bi_{v, gs} = 500$	$H_v = 5.6$
$\Phi_1 = 1\text{--}1.45$	$\Phi_2 = 0.25\text{--}0.36$	
$\zeta_1 = 0.35$	$\zeta_2 = 0.21$	

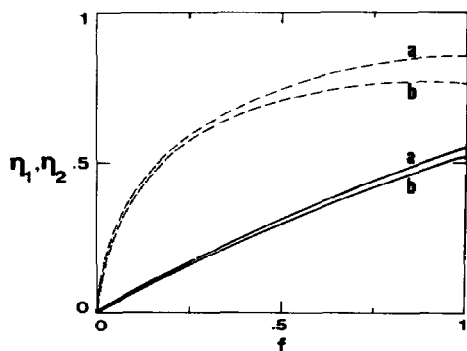


Fig. 11. Effectiveness factor dependence on wetting efficiency for typical hydrodesulphurization conditions of HGO. Curves (a) and (b) correspond to  $\xi_1 = \xi_2 = 1.6$  and  $\xi_1 = \xi_2 = 0.75$  respectively. Polar wetting.

exhibit maxima with respect to  $f$  within the range of  $f$  values (0.7–1) encountered in practice (Colombo *et al.*, 1976; Morita and Smith, 1978; Herskowitz *et al.*, 1979; Mills and Dudukovic, 1981; Herskowitz and Mosseri, 1983). The HDS rate of the less reactive component is maximized at smaller  $f$  values. This is primarily due to its lower diffusivity. Because of mass transfer limitations the effectiveness factor of the more active component is rather low. Computed effectiveness factors are in good qualitative agreement with industrial practice (Cecil *et al.*, 1968; Schuit and Gates, 1973).

#### 4. CONCLUSIONS

A mathematical model has been developed to describe the global kinetic behaviour of reactions between volatile and non-volatile compounds in partially wetted trickle-bed reactor catalyst pellets. Unlike previous studies the analysis assumes no limiting reactant and therefore applies to a number of practical cases where concentrations of dissolved gases and liquid reactants inside the catalyst pellets are comparable. It is shown that the global reaction rate in a pellet is often maximized for intermediate values of the wetting efficiency and thus complete wetting may not be desirable, as interphase mass transport of the gaseous reactant may be seriously hindered. When the ratios  $\xi_1$ ,  $\xi_2$  of volatile to non-volatile components approach zero or infinity, then the present results regarding the role of wetting efficiency are in agreement with previous studies (Mills and Dudukovic, 1979; Mills and Dudukovic, 1980; Herskowitz, 1981b; Goto *et al.*, 1981; Zheng *et al.*, 1984b). For fixed wetting efficiency the number and location of wetted zones also play important roles on catalyst performance. Increasing the length of the wetted zones boundaries, significantly enhances catalyst performance.

The single particle model presented here can be used with arbitrary kinetics to predict the local behaviour in trickle-bed reactors operating in the trickle-flow regime. However when the wetting efficiency of individual particles changes fast with time, as would be the case in the pulse-flow regime, where the pulsing period

(Talmor, 1977) may be comparable to the characteristic diffusion time in the pellets, then steady state models like the one presented here are not applicable and more general dynamic models must be used. Work along this line will be published in a forthcoming communication.

*Acknowledgement*—This work was supported by the Hellenic Refineries of Aspropyrgos, Greece.

#### NOTATION

$Bi_{v, gls}$	Biot number of mass transfer of volatile component at the liquid-covered surface of the particle, $K_{gl, v} d_p / 2D_{e, v}$
$Bi_{v, gs}$	Biot number for mass transfer of volatile component at the gas-covered surface of the particle, $K_{gs, v} d_p / 2D_{e, v}$
$Bi_{S1}, Bi_{S2}$	Biot numbers for mass transfer of non-volatile components S1 and S2 at the liquid-covered surface of the particle, $K_{ls, S1} d_p / 2D_{e, S1}$ , $K_{ls, S2} d_p / 2D_{e, S2}$
$C$	dimensionless concentration
$\bar{C}$	concentration, mole/m <sup>3</sup>
$\bar{C}_{S1, b}, \bar{C}_{S2, b}$	bulk liquid concentrations of S1, S2 components, mole/m <sup>3</sup>
$\bar{C}_{v, b}$	bulk gas concentration of volatile component V, mole/m <sup>3</sup>
$\bar{C}_{v, eq}$	liquid concentration of volatile reactant in equilibrium with its bulk gas concentration, $\bar{C}_{v, b} / H_v$ , mole/m <sup>3</sup>
$D_e$	effective diffusivity in liquid-filled catalyst pellet pores
$d$	density, kg/m <sup>3</sup>
$d_p$	particle diameter, m
$f$	wetting efficiency (external), dimensionless
$H_v$	vapor-liquid equilibrium coefficient of volatile species V, $\bar{C}_{v, b} / \bar{C}_{v, eq}$
$K$	number of computational cells in radial direction
$K_1, K_2$	kinetic constants of reactions (2) and (3) respectively, m <sup>3</sup> /mole s
$K_{ls, S1}, K_{ls, S2}$	liquid to porous solid mass transfer coefficients of nonvolatile reactants S1, S2, m/s
$K_g$	gas film mass transfer coefficient, m/s
$K_L$	liquid film mass transfer coefficient, m/s
$K_s$	liquid to porous solid mass transfer coefficient, m/s
$K_{gl, v}$	overall gas-liquid-porous solid mass transfer coefficient of volatile reactant V at the wetted external pellet surface, m/s
$K_{gs, v}$	overall gas to porous solid mass transfer coefficient of volatile reactant V at the dry external pellet surface

$L$	number of computational cells in angular direction
$L[ ]$	operator defined in eq. (7)
$M$	molecular weight
$P$	pressure, Pa
$r$	radial coordinate, m
$r_1, r_2$	rate of reactions (2) and (3) respectively, mole/m <sup>3</sup> s
$r_1^*, r_2^*$	dimensionless rates of reactions (2) and (3)
$R$	pellet radius, m
$S_1, S_2$	liquid reactants; in the case of HGO high and low reactivity sulphur containing pseudocomponents
$T$	temperature, K
$V_{S_1}, V_{S_2}, V_{H_2}$	molal volumes of reactants $S_1, S_2, H_2$ at normal boiling point, m <sup>3</sup> /gmole
$V$	volatile reactant

## Greek symbols

$\alpha_1, \alpha_2$	stoichiometric coefficients in reactions (2) and (3) respectively
$\epsilon_p$	particle porosity, dimensionless
$\zeta_1, \zeta_2$	effective diffusivity ratios $D_{e,S_1}/D_{e,v}$ , $D_{e,S_2}/D_{e,v}$ respectively
$\eta_1, \eta_2$	effectiveness factors for reactions (2) and (3)
$\eta_L$	effectiveness factors for completely wetted pellet
$\eta_{overall}$	effectiveness factor defined in eq. (16)
$\Theta$	azimuthal angle
$\Theta_f$	wetting angle shown in Fig. 1
$\mu$	viscosity, Pa s
$\xi_1, \xi_2$	ratio of equilibrium volatile to non-volatile reactant concentrations, $\bar{C}_{v,eq}/\bar{C}_{S_1}$ , $\bar{C}_{v,eq}/\bar{C}_{S_2}$ , b
$\rho$	dimensionless radial coordinate, $r/R$
$\Phi_1, \Phi_2$	Thiele moduli for reactants $S_1$ and $S_2$ , defined after eq. (7)

## Subscripts

1, 2	refer to reactions (2) and (3) respectively
b	bulk conditions
g	gas phase
l	liquid phase
L	completely wetted pellet surface

## REFERENCES

- Broderick, D. H., 1980, Ph.D. Thesis, University of Delaware, Newark.
- Broderick, D. H. and Gates, B. C., 1981, Hydrogenolysis and hydrogenation of dibenzothiophene catalyzed by sulfided CoO-MoO<sub>3</sub>/γ-Al<sub>2</sub>O<sub>3</sub>: the reaction kinetics. *A.I.Ch.E. J.* **27**, 663-673.
- Brunner, E., 1985, Solubility of hydrogen in 10 organic solvents at 298.15, 323.15 and 373.15 K. *Chem. Engng Data* **30**, 269-273.
- Capra, V., Sicardi, S., Gianetto, A. and Smith, J. M., 1982, Effect of liquid wetting on catalyst effectiveness in trickle-bed reactors. *Can. J. chem. Engng* **60**, 282-288.
- Cecil, R. R., Mayer, F. X. and Cart, E. N., 1968, paper presented at Am. Inst. Chem. Engrs Meeting, Los Angeles.
- Colombo, A. J., Baldi, G. and Sicardi, S., 1976, Solid-liquid contacting effectiveness in trickle-bed reactors. *Chem. Engng Sci.* **31**, 1101-1108.
- Gates, B. C., Katzer, J. R. and Shuit, G. C. A., 1979, *Chemistry of Catalytic Processes*, pp. 390-443. McGraw-Hill, New York.
- Gianetto, A., Baldi, G., Specchia, V. and Sicardi, S., 1978, Hydrodynamics and solid-liquid contacting effectiveness in trickle-bed reactors. *A.I.Ch.E. J.* **24**, 1087-1104.
- Goto, S. and Smith, J. M., 1975, Trickle-bed reactor performance, Part I: Holdup and mass transfer effects. *A.I.Ch.E. J.* **21**, 706-713.
- Goto, S., Lakota, A. and Levec, J., 1981, Effectiveness factors on nth order kinetics in trickle-bed reactors. *Chem. Engng Sci.* **36**, 157-162.
- Herskowitz, M., 1981a, Effects of wetting efficiency on selectivity in a trickle-bed reactor. *Chem. Engng Sci.* **36**, 1099-1101.
- Herskowitz, M., 1981b, Wetting efficiency in trickle-bed reactors. The overall effectiveness factor of partially wetted catalyst particles. *Chem. Engng Sci.* **36**, 1665-1671.
- Herskowitz, M. and Mosseri, S., 1983, Global rates of reaction in trickle-bed reactors: effects of gas and liquid flow rates. *Ind. Engng Chem. Fundam.* **22**, 4-6.
- Herskowitz, M. and Smith, J. M., 1983, Trickle-bed reactors: a review. *A.I.Ch.E. J.* **29**, 1-18.
- Herskowitz, M., Carbonell, R. G. and Smith, J. M., 1979, Effectiveness factors and mass transfer in trickle-bed reactors. *A.I.Ch.E. J.* **25**, 272-282.
- Houalla, M., Nag, N. K., Sapre, A. V., Broderick, D. H. and Gates, B. C., 1978, Hydrodesulfurization of dibenzothiophene catalyzed by sulfided CoO-MoO<sub>3</sub>/γ-Al<sub>2</sub>O<sub>3</sub>: the reaction network. *A.I.Ch.E. J.* **24**, 1015-1021.
- Houalla, M., Broderick, D. H., Sapre, A. V., Nag, N. K., De Beer, V. H. J., Gates, B. C., and Kwart, H., 1980, Hydrodesulfurization of methyl-substituted dibenzothiophenes catalyzed by sulfided Co-Mo/γ-Al<sub>2</sub>O<sub>3</sub>. *J. Catal.* **61**, 523-527.
- Kumar, M., Akgerman, A. and Anthony, R. G., 1984, Desulfurization by *in situ* hydrogen generation through water gas shift reaction. *Ind. Engng Chem Processes, Des. Dev.* **23**, 88-93.
- Lee, H. H. and Smith, J. M., 1982, Trickle-bed reactors: criteria of negligible transport effects and of partial wetting. *Chem. Engng Sci.* **37**, 223-227.
- Mahajani, V. V. and Sarma, M. M., 1979, Effective interfacial area and liquid-particle mass transfer in trickle-beds. *A.I.Ch.E. J.* **28**, 190-195.
- Mills, P. L. and Dudukovic, M. P., 1979, A dual-series solution for the effectiveness factor of partially wetted catalysts in trickle-bed reactors. *Ind. Engng Chem. Fundam.* **18**, 139-149.
- Mills, P. L. and Dudukovic, M. P., 1980, Analysis of catalyst effectiveness in trickle-bed reactors processing volatile or nonvolatile reactants. *Chem. Engng Sci.* **35**, 2267-2279.
- Mills, P. L. and Dudukovic, M. P., 1981, Evaluation of liquid-solid contacting in trickle-bed reactors by tracer methods. *A.I.Ch.E. J.* **27**, 893-904.
- Morita, S. and Smith, J. M., 1978, Mass transfer and contacting efficiency in a trickle-bed reactors. *Ind. Engng Chem. Fundam.* **17**, 113-120.
- Nag, N. K., Sapre, A. V., Broderick, D. H. and Gates, B. C., 1979, Hydrodesulfurization of polycyclic aromatics catalyzed by sulfide CoO-MoO<sub>3</sub>/γ-Al<sub>2</sub>O<sub>3</sub>: the relative reactivities. *J. Catal.* **57**, 509-512.
- Ramachandran, P. A. and Smith, J. M., 1979, Effectiveness factors in trickle-bed reactors. *A.I.Ch.E. J.* **25**, 538-542.
- Ramanujam, S., Leipziger, S. and Well, S. A., 1985,

Table 3. Computed Thiele moduli  $\Phi_1$ ,  $\Phi_2$  for  $\bar{C}_{S1,b} = \bar{C}_{S2,b} = 2 \times 10^{-4}$  mole/cm<sup>3</sup>

T/K	P/bar	$\Phi_1$	$\Phi_2$	Comments	Reference
625	48	0.4 <sup>†</sup>	0.3 <sup>‡</sup>	<sup>†</sup> LGO <sup>‡</sup> HGO	(Yitzhaki and Aharoni, 1977)
573	71	7.0	1.9		(Nag <i>et al.</i> , 1979)
573	90	—	0.45		(Rollmann, 1977)
617	102	—	1.1–2		(Houalla <i>et al.</i> , 1980)
573	35	—	0.25	Manufacturers data for HDS-16A	

Vapor-liquid equilibrium for a hydrogen/simulated coal-derived liquid system. *Ind. Engng Chem. Process Des. Dev.* **24**, 364–368.

Reid, R. C., Prausnitz, J. M. and Sherwood, T. K., 1977, *The Properties of Gases and Liquids*, 3rd edn. McGraw-Hill, New York.

Ring, Z. E. and Missen, R. W., 1986, Trickle-bed reactors: effect of wetting geometry on overall effectiveness factor. *Can. J. chem. Engng* **64**, 117–124.

Rollmann, L. D., 1977, Catalytic hydrogenation of model nitrogen, sulfur and oxygen compounds. *J. Catal.* **46**, 243–252.

Satterfield, C. N., 1975, Trickle-bed reactors. *A.I.Ch.E. J.* **29**, 1–18.

Satterfield, C. N. and Roberts, G. N., 1968, Kinetics of thiophene hydrogenolysis on a cobalt molybdate catalyst. *A.I.Ch.E. J.* **14**, 159–164.

Satterfield, C. N., Van Eek, M. W. and Bliss, G. S., 1978, Liquid-solid mass transfer in packed beds with downward concurrent gas-liquid flow. *A.I.Ch.E. J.* **24**, 709–717.

Schuit, G. C. A. and Gates, B. C., 1973, Chemistry and engineering of catalytic hydrodesulfurization. *A.I.Ch.E. J.* **19**, 417–438.

Shah, Y. T., 1979, *Gas-Liquid-Solid Reactor Design*. McGraw-Hill, New York.

Singhal, G. H., Espino, R. L., Sobel, J. E. and Huff, G. A., 1981, Hydrodesulfurization of sulfur heterocyclic compounds. Kinetics of dibenzothiophene. *J. Catal.* **67**, 457–468.

Talmor, E., 1977, Two-phase downflow through catalyst beds. Part I: Flow maps. Part II: Pulsing regime pressure drop. *A.I.Ch.E. J.* **23**, 868–878.

Tan, C. S. and Smith, J. M., 1980, Catalyst particle effectiveness with unsymmetrical boundary conditions. *Chem. Engng Sci.* **35**, 1601–1609.

Tan, C. S. and Smith, J. M., 1982, A dynamic method for liquid-particle mass transfer in trickle-beds. *A.I.Ch.E. J.* **28**, 190–195.

Van Landeghem, 1980, Multiphase reactors: mass transfer and modeling. *Chem. Engng Sci.* **35**, 1912–1949.

Vrinat, M. L., 1983, The kinetics of the hydrodesulfurization process—a review. *Appl. Catalysis* **6**, 137–158.

Yentekakis, I. V., 1987, Ph.D. Thesis, University of Patras, Patras.

Yitzhaki, D. and Aharoni, C., 1977, Hydrodesulfurization of gas oil, reaction rates in narrow boiling range fractions. *A.I.Ch.E. J.* **23**, 342–346.

Zheng Lu, P., Smith, J. M. and Herskowitz, M., 1984a, Gas-particle mass transfer in trickle-beds. *A.I.Ch.E. J.* **30**, 500–502.

Zheng Lu, P., Han-Yu, F. and Smith, J. M., 1984b, Trickle-bed effectiveness factors for liquid-phase reactants. *A.I.Ch.E. J.* **30**, 818–820.

## APPENDIX

### PARAMETER ESTIMATION FOR HDS OF HGO

Diffusivities were computed using the Wilke-Chang correlation (Reid *et al.*, 1977) with  $V_{S1} = 80.8$  cm<sup>3</sup>/mole (Reid *et al.*, 1977),  $V_{S2} = 190$  cm<sup>3</sup>/mole (Yitzhaki and Aharoni, 1977),  $V_{H_2} = 14.3$  cm<sup>3</sup>/mole (Reid *et al.*, 1977). Effective diffusivities were computed assuming a porosity/tortuosity factor of 0.1 (Yitzhaki and Aharoni, 1977).

Gas-liquid mass transfer coefficients for H<sub>2</sub> were computed from the trickle-flow regime correlations of Goto and Smith (1975), which agreed within 30% with the values predicted by the correlation of Mahajani and Sharma (1979).

Liquid-solid mass transfer coefficients for volatile and nonvolatile components were computed from the correlation of Satterfield *et al.* (1978). These values differed less than 40% from those predicted by the equation of Tan and Smith (1982).

The overall gas-liquid-solid mass transfer coefficient of hydrogen  $K_{gls,H_2}$  at the wet catalyst surface was computed from Ramachandran and Smith (1979), and Mills and Dudukovic (1980), i.e.

$$\frac{1}{K_{gls,H_2}} = \frac{1}{K_g H_{H_2}} + \frac{1}{K_L} + \frac{1}{K_S} \quad (A1)$$

where the first RHS term of equation (A1) was, as usual (Herskowitz and Smith, 1983), neglected. The overall gas-solid mass transfer coefficient  $K_{gs,H_2}$  at the dry catalyst surface was taken to be a factor of ten higher than  $K_{gls,H_2}$  (Zheng Lu *et al.*, 1984a).

Due to the lack of direct experimental data for the solubility of H<sub>2</sub> in HGO, this parameter was estimated from literature data on the solubility of H<sub>2</sub> in simulated coal derived liquids (Ramanujam *et al.*, 1985). This approximation is reasonable in view of the fact that the two liquids have several major components in comparable concentrations (Ramanujam *et al.*, 1985). Extrapolating the data of Ramanujam *et al.* (1985) to the operating conditions ( $P = 90$  bar,  $T = 345^\circ\text{C}$ ) one obtains  $X_{H_2,eq} = 0.11$  in reasonable agreement with the data of Broderick (1980) and with the extrapolated value of H<sub>2</sub> solubility in n-decane  $X_{H_2,eq} = 0.15$  (Brunner, 1985) at these conditions.

Thiele moduli were computed on the basis of published kinetic data (Rollmann, 1977; Yitzhaki and Aharoni, 1977; Nag *et al.*, 1979; Houalla *et al.*, 1980) and of data provided by the manufacturers of the commercial catalyst HDS-16A. There is considerable scattering in the kinetic data as shown in Table 3. The Thiele moduli values used in the numerical simulation are shown in Table 2. Further details on the parameter estimation calculations can be found elsewhere (Yentekakis, 1987).